Nonlinear Optical Properties of XPh4 (X = B−, C, N+, P+): A New Class of Molecules with a Negative Third−Order Polarizability

7 AUTHORS, INCLUDING:

Rebecca L. Gieseking
Northwestern University
12 PUBLICATIONS **52** CITATIONS

SEE PROFILE

Trenton R. Ensley
University of Central Florida
31 PUBLICATIONS **171** CITATIONS

SEE PROFILE

Chad Risko
University of Kentucky
93 PUBLICATIONS **2,512** CITATIONS

SEE PROFILE

Eric Van Stryland
University of Central Florida
439 PUBLICATIONS **13,489** CITATIONS

SEE PROFILE

Nonlinear Optical Properties of X(C$_6$H$_5$)$_4$ (X = B$^-$, C, N$^+$, P$^+$): A New Class of Molecules with a Negative Third-Order Polarizability

Rebecca L. Gieseking,[†] Trenton R. Ensley,[‡] Honghua Hu,[‡] David J. Hagan,[‡] Chad Risko,[†,§] Eric W. Van Stryland,*[,‡] and Jean-Luc Brédas*[,†,∥]

[†]School of Chemistry and Biochemistry and Center for Organic Photonics and Electronics, Georgia Institute of Technology, Atlanta, Georgia 30332-0400, United States

[‡]CREOL, The College of Optics and Photonics, University of Central Florida, Orlando, Florida 32816, United States

[§]Department of Chemistry and Center for Applied Energy Research, University of Kentucky, Lexington, Kentucky 40506-0055, United States

[∥]Division of Physical Sciences and Engineering and Solar & Photovoltaics Engineering Research Center, King Abdullah University of Science and Technology, Thuwal 23955-6900, Kingdom of Saudi Arabia

Ⓢ *Supporting Information*

ABSTRACT: Organic π-conjugated materials have been widely used for a variety of nonlinear optical (NLO) applications. Molecules with negative real components Re(γ) of the third-order polarizability, which leads to nonlinear refraction in macroscopic systems, have important benefits for several NLO applications. However, few organic systems studied to date have negative Re(γ) in the long wavelength limit, and all inorganic materials show positive nonlinear refraction in this limit. Here, we introduce a new class of molecules of the form X(C$_6$H$_5$)$_4$, where X = B$^-$, C, N$^+$, and P$^+$, that have negative Re(γ). The molecular mechanism for the NLO properties in these systems is very different from those in typical linear conjugated systems: These systems have a band of excited states involving single-electron excitations within the π-system, several of which have significant coupling to the ground state. Thus, Re(γ) cannot be understood in terms of a simplified essential-state model and must be analyzed in the context of the full sum-over-states expression. Although Re(γ) is significantly smaller than that of other commonly studied NLO chromophores, the introduction of a new molecular architecture offering the potential for a negative Re(γ) introduces new avenues of molecular design for NLO applications.

A new organic-based molecular architecture with negative Re(γ)

X = B$^-$, C, N$^+$, P$^+$
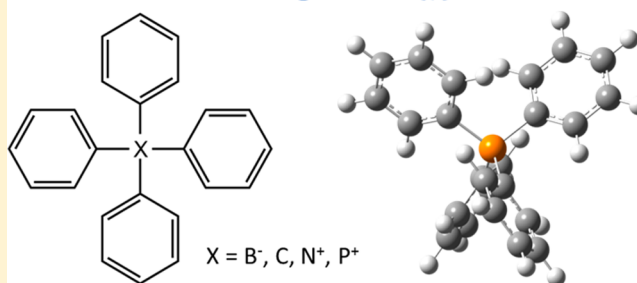
1. INTRODUCTION

Materials based on organic π-conjugated chromophores have been successfully applied in many nonlinear optical (NLO) applications. For instance, molecules with large second-order polarizabilities have been used in electro-optic[1−4] and second-harmonic imaging applications,[5,6] while materials with large imaginary parts of the third-order polarizability have been used in two-photon imaging[7−9] and optical power limiting.[10,11] However, the development of organic materials for applications such as (i) all-optical switching (AOS), which requires very large real parts of the molecular third-order polarizability |Re(γ)| and small imaginary parts Im(γ), or (ii) data transmission, which requires extremely small Re(γ) and Im(γ), has been limited due to challenges in achieving both the necessary molecular and materials properties. Re(γ) is directly proportional to the nonlinear refractive index (n_2) of the material, whereas Im(γ) is directly proportional to the two-photon absorption (2PA) coefficient.

The development of molecules and materials with negative Re(γ) is critical for both AOS and data transmission applications. For AOS applications, few molecular materials have the required figure-of-merit (|Re(γ)/Im(γ)| > 4π).[12−14] Although AOS devices can in principle be made using materials with either a positive or negative value of Re(γ), in practice a negative Re(γ) can provide important benefits. Since materials with positive Re(γ) are self-focusing,[15−17] the peak intensity of each light signal increases as the pulse travels through the material. This limits the laser intensity that can be used without risking dielectric breakdown of the NLO material.[18] As the change in refractive index is linearly dependent on the intensity of light, reducing light intensity would require a larger Re(γ) or a longer interaction length for a functional device. Materials with negative Re(γ) are self-defocusing, which may alleviate these challenges.

A

While large nonlinearities in fibers are required for applications such as AOS, such effects are detrimental for data transmission and for fiber lasers.[19,20] As an example, one can consider liquid core optical fibers (LCOFs). Since the solutions typically used in the cores have positive n_2, the propagation of high intensity pulses in these fibers can induce self-phase modulation (SPM)[21−23] that can spectrally broaden the pulses and eventually lead to supercontinuum generation.[24,25] By doping the core with a small amount of a negative Re(γ) material, the deleterious effects of SPM can be drastically reduced with negligible effects on the linear refractive index.

Although molecules and materials possessing negative Re(γ), and hence negative n_2, could provide substantial benefits for several device applications, to date relatively few classes of materials have been shown to have negative Re(γ).[26−34] Without exception, inorganic materials show positive n_2 in the long wavelength limit,[35,36] leaving organic materials as the sole route to materials with negative n_2. Developing new classes of molecules with negative Re(γ) requires an understanding of the molecular processes that affect the sign and magnitude of γ. The molecular polarizabilities can be described in terms of the response of the molecules to the electric field of light. When an electric field $\vec{F}$ is applied, the molecular dipole moment $\vec{\mu}$ can be expressed in a power series expansion as

$$\vec{\mu}(\vec{F}) = \vec{\mu}_0 + \alpha\cdot\vec{F} + \beta\cdot\vec{F}\vec{F} + \gamma\cdot\vec{F}\vec{F}\vec{F} + \cdots \quad (1)$$

where $\vec{\mu}_0$ represents the permanent molecular dipole moment in the absence of an applied electric field; α, the linear polarizability; and β, the second-order polarizability. If the electric field of light is treated as a perturbation, γ can be expressed in terms of the molecular properties as a sum-over-(electronic) states (SOS) expression:[37]

$$\gamma_{ijkl}(\omega = [\omega_p + \omega_q + \omega_r]; \omega_p, \omega_q, \omega_r) \quad (2)$$

$$= I_{p,q,r}$$

$$\times \left\{ \sum_{u\neq g}\sum_{v\neq g}\sum_{w\neq g} \left[\frac{\langle\psi_g|\hat{\mu}^i|\psi_u\rangle\langle\psi_u|\bar{\mu}^l|\psi_v\rangle\langle\psi_v|\bar{\mu}^k|\psi_w\rangle\langle\psi_w|\hat{\mu}^j|\psi_g\rangle}{(E_{gu}-i\Gamma_{gu}-\hbar\omega)(E_{gv}-i\Gamma_{gv}-\hbar\omega_p-\hbar\omega_q)(E_{gw}-i\Gamma_{gw}-\hbar\omega_p)} \right.\right.$$

$$+ \frac{\langle\psi_g|\hat{\mu}^l|\psi_u\rangle\langle\psi_u|\bar{\mu}^i|\psi_v\rangle\langle\psi_v|\bar{\mu}^k|\psi_w\rangle\langle\psi_w|\hat{\mu}^j|\psi_g\rangle}{(E_{gu}-i\Gamma_{gu}+\hbar\omega_r)(E_{gv}-i\Gamma_{gv}-\hbar\omega_p-\hbar\omega_q)(E_{gw}-i\Gamma_{gw}-\hbar\omega_p)}$$

$$+ \frac{\langle\psi_g|\hat{\mu}^j|\psi_u\rangle\langle\psi_u|\bar{\mu}^k|\psi_v\rangle\langle\psi_v|\bar{\mu}^i|\psi_w\rangle\langle\psi_w|\hat{\mu}^l|\psi_g\rangle}{(E_{gu}-i\Gamma_{gu}+\hbar\omega_p)(E_{gv}-i\Gamma_{gv}+\hbar\omega_p+\hbar\omega_q)(E_{gw}-i\Gamma_{gw}-\hbar\omega_r)}$$

$$+ \left. \frac{\langle\psi_g|\hat{\mu}^j|\psi_u\rangle\langle\psi_u|\bar{\mu}^k|\psi_v\rangle\langle\psi_v|\bar{\mu}^l|\psi_w\rangle\langle\psi_w|\hat{\mu}^i|\psi_g\rangle}{(E_{gu}-i\Gamma_{gu}+\hbar\omega_p)(E_{gv}-i\Gamma_{gv}+\hbar\omega_p+\hbar\omega_q)(E_{gw}-i\Gamma_{gw}+\hbar\omega)} \right]$$

$$- \sum_{u\neq g}\sum_{w\neq g} \left[\frac{\langle\psi_g|\hat{\mu}^i|\psi_u\rangle\langle\psi_u|\hat{\mu}^l|\psi_g\rangle\langle\psi_g|\hat{\mu}^k|\psi_w\rangle\langle\psi_w|\hat{\mu}^j|\psi_g\rangle}{(E_{gu}-i\Gamma_{gu}-\hbar\omega)(E_{gu}-i\Gamma_{gu}-\hbar\omega_r)(E_{gw}-i\Gamma_{gw}-\hbar\omega_p)} \right.$$

$$+ \frac{\langle\psi_g|\hat{\mu}^i|\psi_u\rangle\langle\psi_u|\hat{\mu}^l|\psi_g\rangle\langle\psi_g|\hat{\mu}^k|\psi_w\rangle\langle\psi_w|\hat{\mu}^j|\psi_g\rangle}{(E_{gu}-i\Gamma_{gu}-\hbar\omega_r)(E_{gw}-i\Gamma_{gw}+\hbar\omega_q)(E_{gw}-i\Gamma_{gw}-\hbar\omega_p)}$$

$$+ \frac{\langle\psi_g|\hat{\mu}^l|\psi_u\rangle\langle\psi_u|\hat{\mu}^i|\psi_g\rangle\langle\psi_g|\hat{\mu}^j|\psi_w\rangle\langle\psi_w|\hat{\mu}^k|\psi_g\rangle}{(E_{gu}-i\Gamma_{gu}+\hbar\omega)(E_{gu}-i\Gamma_{gu}+\hbar\omega_r)(E_{gw}-i\Gamma_{gw}+\hbar\omega_p)}$$

$$+ \left.\left. \frac{\langle\psi_g|\hat{\mu}^l|\psi_u\rangle\langle\psi_u|\hat{\mu}^i|\psi_g\rangle\langle\psi_g|\hat{\mu}^j|\psi_w\rangle\langle\psi_w|\hat{\mu}^k|\psi_g\rangle}{(E_{gu}-i\Gamma_{gu}+\hbar\omega_r)(E_{gw}-i\Gamma_{gw}-\hbar\omega_q)(E_{gw}-i\Gamma_{gw}+\hbar\omega_p)} \right]\right\}$$

where the $\hbar\omega_{p,q,r}$ terms denote the photon energies; g, the electronic ground state; u, v, and w, the electronic excited states; E_{gu}, the transition energy from state g to state u; $\hat{\mu}^j$, the electric dipole moment operator along molecular axis j; $\bar{\mu}^j$, the transition dipole moment between states u and v only if u and v are different, or if u and v are the same, then $\bar{\mu}^j$ is the difference

between the state dipole moments of state u and the ground state; i, the imaginary unit; Γ_{gu}, a damping factor for excited state u, which is related to the excited-state lifetime; and $I_{p,q,r}$, the average over the terms obtained by simultaneous permutation of the incident photon frequency and the dipole moment operator. In molecular systems where only one excited state is strongly coupled to the ground state and the primary components of the state dipole moments and transition dipole moments are aligned along one molecular axis x, the full SOS expression can be simplified to an essential-state model with three terms,[38−43] which in the static limit appears as

$$\gamma_{xxxx} \propto \frac{\mu_{ge}^2\Delta\mu_{eg}^2}{E_{ge}^3} \qquad \mathbf{D}$$

$$+ \sum_{e'} \frac{\mu_{ge}^2\mu_{ee'}^2}{E_{ge}^2 E_{ge'}} \qquad \mathbf{T}$$

$$- \frac{\mu_{ge}^4}{E_{ge}^3} \qquad \mathbf{N} \qquad (3)$$

The three terms are denoted $\mathbf{D}$ (for dipolar term, which is only nonzero in noncentrosymmetric systems), $\mathbf{T}$ (for two-photon term, which derives from the fact that in centrosymmetric systems this term involves transitions from the one-photon excited state e to two-photon excited states e′), and $\mathbf{N}$ (for negative term, due to the minus sign in front of the term).

In linear π-conjugated systems such as cyanines,[27,44−46] donor−acceptor-substituted polyenes,[26,27,44] and squaraines,[28,31] molecular design principles describing the sign and magnitude of Re(γ) have been developed through understanding the relationship between the nature of the first several excited states and the geometric parameters related to bond-length alternation (BLA) along the π backbone. However, this molecular understanding of Re(γ) has not yet been extended to higher-dimensional systems where the application of the essential-state model is not expected to be applicable.

Here, we present a new class of molecules with negative Re(γ):tetraphenyl compounds $X(C_6H_5)_4$, where X = B$^-$, C, N$^+$, and P$^+$ (Figure 1). We first describe the geometric and
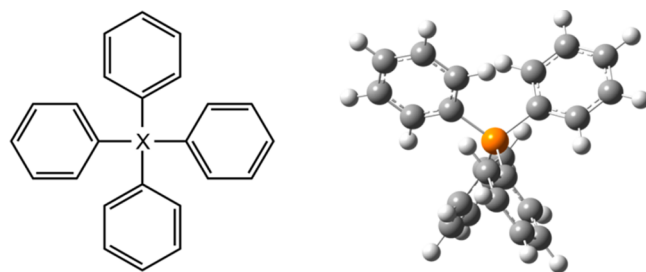

Figure 1. General chemical structure of the XPh$_4$ series (X = B$^-$, C, N$^+$, P$^+$) and sketch of the geometric structure of PPh$_4^+$.

electronic structures of these molecules, which have three-dimensional π systems and do not correspond with the geometric parameters typically used to understand the sign of Re(γ) in linear conjugated systems. We then discuss the excited-state properties and NLO properties and demonstrate that the sign and magnitude of Re(γ) can be understood only in terms of the properties of a band of excited states in the context of the full SOS model. Finally, we present experimental

confirmation that $\text{Re}(\gamma)$ at the static limit is indeed negative in these systems.

2. METHODS

2.1. Computational Methodology. The geometric structures were optimized via density functional theory (DFT) using the ωB97XD functional[47,48] and cc-pVDZ basis set[49] as implemented in the Gaussian 09 (Rev. B.01) suite of programs.[50] All geometry minima were confirmed by the absence of imaginary frequencies. As the molecules have S_4 symmetry, the z axis was defined as the axis of symmetry. The excited-state properties were then evaluated using a configuration interaction (CI) approach using single-electron excitations (SCI) with the INDO Hamiltonian;[27,51,52] this approach has previously provided excellent agreement with the experimental NLO properties of π-conjugated systems.[53,54] The CI active space included all single-electron excitations within the 25 highest-lying occupied molecular orbitals (MOs) and 25 lowest-lying unoccupied MOs. Although double-electron excitations are usually critical to accurately compute the low-lying excited state properties of π-conjugated systems,[51,53,55–57] test calculations incorporating double-electron excitations through SDCI (single and double CI) or MRDCI (multireference determinant CI) schemes show that the first 40–60 excited states in these systems contain negligible double-excitation character; hence, excitations with such character can be safely neglected through use of the SCI approach.

The NLO properties were computed using the sum-over-states approach (power series expansion). The total static $\text{Re}(\gamma)$ and $\text{Im}(\gamma)$ evaluated by summing over 100 states. Decomposition of the contributions from each of the excited states was achieved by calculating the static γ value separately for each state u in eq 2. The static γ was also decomposed into contributions from the **D**, **T**, and **N** terms; in doing so, the first summation in the full SOS expression, comprises the **D** (u = v = w) and **T** (u $\neq$ v and/or v $\neq$ w) terms and the second summation comprises the **N** term. The orientationally averaged $\text{Re}(\gamma)$ is computed from the tensor components as

$$\gamma_{avg} = \frac{1}{5}(\gamma_{xxxx} + \gamma_{yyyy} + \gamma_{zzzz}) + \frac{1}{15}(\gamma_{xxyy} + \gamma_{yyxx} + \gamma_{xyyx} + \gamma_{xyxy}$$
$$+ \gamma_{yxyx} + \gamma_{yxxy} + \gamma_{xxzz} + \gamma_{zzxx} + \gamma_{xzzx} + \gamma_{xzxz} + \gamma_{zxzx}$$
$$+ \gamma_{zxxz} + \gamma_{zzyy} + \gamma_{yyzz} + \gamma_{zyyz} + \gamma_{zyzy} + \gamma_{yzyz} + \gamma_{yzzy}) \quad (4)$$

2.2. Experimental Methodology. The linear absorption of PPh_4^+ dissolved in spectroscopic grade chloroform was measured using a Varian Cary 500 spectrophotometer. To study the possible effects of aggregation, we prepared solutions ranging from concentrations of 22 μM up to 91 mM and measured their absorption spectra in quartz cuvettes with thicknesses varying from 1 cm to 0.01 mm, respectively.

To measure the $\text{Re}(\gamma)$ far from the one-photon absorption resonance, we used the recently developed dual-arm (DA) Z-scan technique,[58] an extension of the conventional Z-scan method.[59] The DA Z-scan technique allows for the simultaneous subtraction of the solvent nonlinear signal from the solution. For simultaneous subtraction, the two arms are identically matched in terms of the irradiance parameters, i.e., pulse energy, beam waist, pulse width, and sample positioning, and as a result, the correlated noise from the excitation source is canceled. This leaves only the nonlinear signal due to the solute with a large increase in the signal-to-noise ratio. This significantly improves our ability to measure the $\text{Re}(\gamma)$ when approaching the static limit where the nonlinear refraction is small. In this regime, the typically large signal from the solvent can mask that due to the solute. Furthermore, the $\text{Im}(\gamma)$, corresponding to NLO losses, is essentially zero far from resonance, thus the DA Z-scan signals presented in the subsequent section are solely attributed to $\text{Re}(\gamma)$.

3. RESULTS AND DISCUSSION

3.1. Computational Results. *3.1.1. Ground-State Properties.* We start by discussing the geometric and electronic

structures of the series of tetraphenyl compounds $X(C_6H_5)_4$, where X = B$^-$, C, N$^+$, and P$^+$; note that XPh_4 will be used throughout to simplify the nomenclature for these structures. All of these systems have energetic minima in geometries with S_4 symmetry. The bond lengths within the phenyl rings are similar across the series, and the rings maintain the aromatic character associated with isolated benzene rings. This can be seen through analysis of the quinoidal-benzene character (QBC), defined as $\sum_i(|r_i - 1.4\text{ Å}|)$, where r_i is the length of each C−C bond i in the phenyl ring.[28] The QBC values for these compounds are all very small (<0.05 Å; we note that for squaraines, the crossover point from aromatic-like structures with positive $\text{Re}(\gamma)$ to quinoid-like structures with negative $\text{Re}(\gamma)$ was computed to be on the order of 0.17 Å).[28] This indicates that the phenyl rings largely retain their aromatic character; the quinoidal form has a minimal contribution to the ring conjugation pattern. It is useful to recall at this stage that the negative $\text{Re}(\gamma)$ in cyanines and squaraines can be attributed to the molecule being in an intermediate geometry between two resonance forms, where the ground state is highly polarizable, more so than any low-lying excited state. In the XPh_4 series, the nature of the molecular geometries suggests that the negative $\text{Re}(\gamma)$ cannot be attributed to the same cause.

The frontier MOs in the XPh_4 series are π-orbitals. The eight highest occupied MOs (HOMOs) are composed of linear combinations of the two highest occupied orbitals of each of the four phenyl rings; similarly, the eight lowest unoccupied MOs (LUMOs) are composed of linear combinations of the two lowest unoccupied orbitals of each phenyl ring (representations of the MOs are provided in the SI). In all members of the series, the HOMO is doubly degenerate, whereas the LUMO is nondegenerate. The nondegenerate MOs are fully delocalized across all four phenyl rings (in the degenerate MO pairs, the total electron density of the two orbitals can also be seen as distributed evenly across all four phenyl rings). Because the coupling between the orbitals on different phenyl rings is small, the energetic spacing within each of these sets of eight MOs is small enough to effectively form bands of occupied and unoccupied π-orbitals (Figure 2). Such an electronic structure is markedly different from that seen in most linear π-conjugated systems, which typically have significant energetic gaps separating frontier MOs. Since the central atom has little contribution to the frontier MOs, the HOMO−LUMO gap is relatively unaffected by changes to the
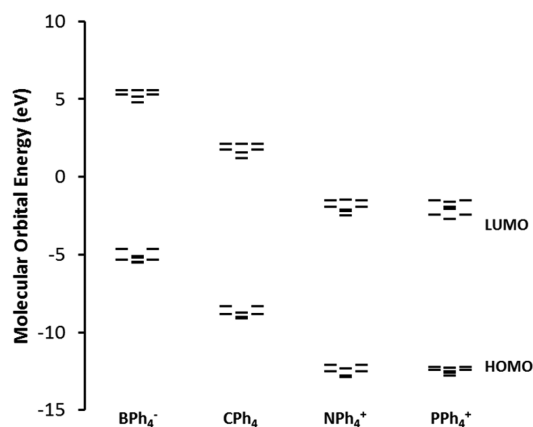

Figure 2. Molecular orbital energies (HOMO−7 through LUMO+7) at the INDO level in the XPh_4 series.

Table 1. State Energies, Key Dipole Moment Parameters, and CI Composition of Excited States of PPh₄⁺[a]

state	energy (eV)	$\Delta\mu_{eg}$ (Debye)	μ_{ge} (Debye)	CI composition
17	6.44	$-0.57\ z$	$-5.47\ x - 0.28\ y$	$-0.32|H{-}4 \rightarrow L{+}4\rangle - 0.32|H{-}4 \rightarrow L{+}5\rangle + 0.43|H{-}1 \rightarrow L\rangle$ $- 0.32|H \rightarrow L{+}1\rangle$
18	6.44	$0.57\ z$	$0.28\ x - 5.47\ y$	$-0.32|H{-}4 \rightarrow L{+}4\rangle - 0.32|H{-}4 \rightarrow L{+}5\rangle + 0.32|H{-}1 \rightarrow L{+}1\rangle$ $+ 0.43|H \rightarrow L\rangle$
19	6.45	0	$-6.80\ z$	$+0.34|H{-}6 \rightarrow L{+}5\rangle - 0.33|H{-}4 \rightarrow L{+}7\rangle + 0.33|H{-}3 \rightarrow L{+}6\rangle$ $- 0.34|H{-}2 \rightarrow L{+}4\rangle$
20	6.47	$-6.27\ z$	$-5.94\ x - 3.93\ y$	$-0.53|H{-}1 \rightarrow L\rangle - 0.42|H{-}1 \rightarrow L{+}1\rangle$
21	6.47	$6.27\ z$	$-3.93\ x + 5.94\ y$	$+0.53|H \rightarrow L\rangle - 0.42|H \rightarrow L{+}1\rangle$
31	6.82	0	$-5.40\ z$	$+0.50|H{-}5 \rightarrow L\rangle - 0.36|H{-}4 \rightarrow L{+}3\rangle + 0.36|H{-}3 \rightarrow L{+}2\rangle$

[a]All excited states within the first 100 states with $\mu_{ge} > 4$ D are listed, and x, y, and z denote the molecular axes, where z is the axis of symmetry.

central atom, and its calculated value varies only between 9.44 eV (B⁻) and 9.61 eV (N⁺) within the series.

3.1.2. Excited-State Properties. We now turn to the excited-state energies, configuration interaction compositions, and state dipole and transition dipole moments. This discussion will center on how the first several frontier MOs determine the low-lying excited-state properties. As the MOs and excited-state properties do not change substantially among the members of this series, we have chosen here to focus on PPh₄⁺. Because the frontier MOs have the band-like energetic spacing discussed in the previous section, the compositions of the XPh₄ excited states are much more complex than those of typical linear π-conjugated systems. The first several excited states have little one- or two-photon activity; instead, the optical and NLO properties are dependent on many higher-lying states, as will be discussed in more detail in the following paragraphs. Understanding the general trends in the energies and transition dipole moments among many excited states is critical to understanding the molecular optical and NLO properties.

Because of the relatively small energetic gaps among the first eight HOMOs and the first eight LUMOs, the single-electron excitations within this range of MOs are all relatively similar in energy (a total of 64 single excitations) and are energetically well-separated from any other excitations within the π-system. The first 40−60 excited states are composed of linear combinations of these low-lying single excitations, with negligibly small contributions from higher-energy excitations (Table 1). The first excited state has an energy of 4.64 eV; however, we focus here on the higher-lying excited states within this band that are more strongly coupled to the ground state. Each excited state is composed of a linear combination of many single excitations; in only a few excited states does any one excitation compose more than 30% of the state electronic configuration (CI coefficient = 0.55).

We note that the excited states exhibit symmetry-breaking if their geometries are allowed to relax. In particular, at the CIS level, the C_1-optimized structure of the first excited state is stabilized by 0.1 eV as compared to the S_4-optimized geometry. The geometric changes in the C_1 geometry suggest that the excitation becomes localized primarily on one phenyl ring; one P−C bond is shortened by 0.04 Å, and the C−C bonds in that phenyl ring are lengthened by 0.03 Å relative to the other three phenyl rings. However, the electronic NLO processes occur substantially faster than geometric relaxations and involve the excited states as virtual states. Thus, here, we focus solely on the excited-state properties in the S_4 ground-state geometry.

To understand the state dipole moments and the transition dipole moments, we first consider the contributions of the pure single-electron excitations and then evaluate the effect of the linear combinations of excitations in the excited states. We turn first to the state dipole moments. In the ground state, the S_4 molecular symmetry implies that the dipole moment μ_g is zero;[60] thus, the difference $\Delta\mu_{eg}$ between the excited-state and ground-state dipole moments is equal to the excited-state dipole moment μ_e. The excited-state dipole moments depend on the electron distribution, related to the MO spatial distributions. Since most of the MOs are symmetrically distributed across the molecule, the single excitations between these orbitals do not change the molecular dipole moment. However, in transitions involving MOs in degenerate pairs, the two transitions involving each orbital in the pair will have state dipole moments along the molecular z axis that are equal in magnitude but opposite in sign.

The excited-state dipole moments μ_e can be considered as weighted sums of the changes in the state dipole moment due to each component electronic configuration. If an excited state only involves transitions among non-degenerate orbitals, all excitations have contributions of zero to μ_e; thus, the total μ_e must be equal to zero. If the contributions from pairs of degenerate excitations are equal in magnitude, the contributions to the state dipole moment cancel and $\mu_e = 0$. However, if the contributions from degenerate excitations are not equal, as happens in pairs of degenerate excited states, μ_e can be as large as 6 D; within each pair of degenerate states, the two μ_e values are equal in magnitude but opposite in sign.

For each excited state e, the transition dipole moment μ_{ge} to the ground state is likewise composed of a linear combination of contributions from each component excitation. The upper eight HOMOs are composed of linear combinations of the phenyl orbitals that have one node within each phenyl ring, whereas the lower eight LUMOs are composed of linear combinations of the phenyl orbitals that have two nodes within each phenyl ring. In each excitation from one of the first eight HOMOs to one of the first eight LUMOs, the differing number of nodes within each phenyl ring implies that each ring has some atoms where the transition density has a positive sign and some where the transition density has a negative sign. The cancellation of positive and negative transition densities within each phenyl ring limits the magnitude of the orbital transition dipole moments. The orbital components of the transition dipole moments are therefore relatively small, ranging from 0 to

4 D,[61] and may be aligned either along the molecular z axis or in the xy plane.

Since the low-lying excited states are composed of single excitations, the transitions from the ground state to each CI component in each excited state all involve electronic configurations that are different by one orbital. Thus, the transition dipole moments μ_{ge} can be computed as linear combinations of the transition dipole moments of all component excitations. Depending on the signs of the CI coefficients and the orbital transition dipole moments, the components can combine additively or subtractively. Several excited states have significant μ_{ge} (Table 1); as will be detailed later, these states give the most significant contributions to the linear and NLO properties. Notably, there are states with large μ_{ge} both along the molecular z axis and in the xy plane. This is different from typical linear π-conjugated molecules, which commonly have only one low-lying excited state that is significantly coupled to the ground state.[27]

The transition dipole moments $\mu_{\mathrm{ee}'}$ between excited states involve linear combinations of transitions between singly excited electron configurations. Since only transitions between configurations that differ by no more than one orbital can have nonzero contributions to the transition dipole moment, only configuration pairs in which the excitations involve either the same occupied orbital or the same unoccupied orbital can contribute to $\mu_{\mathrm{ee}'}$. An allowed transition between two singly excited configurations therefore involves a one-electron transition within either the occupied manifold or the unoccupied manifold. The transitions between two HOMOs or between two LUMOs can have much larger orbital transition dipole moments than the transitions between one HOMO and one LUMO because the transition densities within each ring can all contribute with the same sign to the transition dipole moment. The orbital components of the transition dipole moments range from 0 to 9 D, up to a factor of two larger than for the HOMO−LUMO transitions; again, these components can be aligned either along the z axis or in the xy plane.

Even though the orbital contributions to $\mu_{\mathrm{ee}'}$ are large, the significant mixing of excitations in each excited state limits the magnitude of $\mu_{\mathrm{ee}'}$. Most pairs of excitations differ by two orbitals and have no contribution to $\mu_{\mathrm{ee}'}$. In configuration pairs that do contribute to $\mu_{\mathrm{ee}'}$, the orbital component is multiplied by two relatively small CI coefficients (as noted previously, typically <0.55), so only infrequently does any one configuration pair contribute more than 1 D to $\mu_{\mathrm{ee}'}$. In transitions with multiple configuration pairs contributing to $\mu_{\mathrm{ee}'}$, the terms may contribute additively or subtractively. Importantly, the excited states that are strongly coupled to the ground state have few large transition dipole moments to other excited states (Table 2). This weak coupling between excited states implies

Table 2. Transition Dipole Moments between Excited States in PPh$_4$$^{+a}$

transition	$\mu_{\mathrm{ee}'}$ (Debye)
19 → 25	4.94 z
20 → 23	5.50 z
20 → 25	2.76 x + 3.44 y
21 → 24	5.50 z
21 → 25	3.44 x − 2.76 y

^{a}All transition dipole moments greater than 4 D from the states listed in Table 1 to other excited states are listed.

that there is relatively little 2PA in these systems; as will be described in the following section, this also has important implications in determining the sign of Re(γ).

3.1.3. Nonlinear Optical Properties. We can understand the negative sign of Re(γ) in terms of the excited-state energies, state dipole moments, and transition dipole moments. As will be discussed in the following section, the magnitude and sign of the computed Re(γ) are in good agreement with the experimental results. Here, we focus on Re(γ) at the static (zero-frequency) limit. As mentioned previously, because there are several excited states with large coupling to the ground state along different molecular axes, the commonly used essential-state model cannot be applied to these systems. Instead, we discuss the NLO properties in terms of the full SOS expression (eq 2). Although this expression might at first look complex, we recall that each term simply consists of a product of four transition dipole and/or state dipole terms in the numerator and a product of three state-energy terms in the denominator.

To provide insight into the origins of the NLO properties, we decompose γ into contributions from each one-photon state u in eq 2. As Im(γ) is negligibly small at the static limit, we focus solely on Re(γ). The Re(γ) values presented here are orientationally averaged as described in eq 4; unlike in linear π-conjugated systems, the total Re(γ) is nearly isotropic in these systems because there are large μ_{ge} terms along all three molecular axes. As shown in Table 3, Re(γ) contains significant contributions from a number of excited states, particularly those that are strongly coupled to the ground state.

Table 3. Re(γ) and Its Major State Components and Term Decomposition of PPh$_4$$^+$ ($\times$ 10^{-36} esu)^a

state	total	**D**	**T**	**N**
17	−3.3	0.0	0.7	−4.0
18	−3.3	0.0	0.7	−4.0
19	−5.4	0.0	0.7	−6.1
20	−5.9	0.5	0.2	−6.6
21	−5.9	0.5	0.2	−6.6
31	−3.2	0.0	0.3	−3.5
total	−39.8	1.1	2.1	−43.0

^{a}All states with total contributions >2 $\times$ 10^{-36} esu are included.

We also consider the contributions to Re(γ) from each of the three terms as decomposed in the essential-state model. Because the excited states with significant contributions to Re(γ) all fall within a relatively narrow energy window, the denominators of all terms are similar in magnitude, and we can focus on the numerators. The second summation in the full SOS expression (corresponding to the **N** term in the essential-state model) contains a product of four μ_{ge} terms in the numerator. Although the essential-state model simplifies this term to the form $-\mu_{\mathrm{ge}}^4/E_{\mathrm{ge}}^3$, the full SOS expression also includes terms of the form $-(\mu_{\mathrm{gu}}^2\mu_{\mathrm{gw}}^2)/(E_{\mathrm{gu}}^2 E_{\mathrm{gw}})$, where u and w are both excited states. When multiple excited states are significantly coupled to the ground state, these cross-terms have significant contributions to Re(γ). Because the XPh$_4$ systems have several excited states that are coupled to the ground state, these terms have a significant negative contribution to Re(γ).

The first summation in the SOS expression has an additional dependence on the transition dipole moments $\mu_{\mathrm{ee}'}$ between excited states (**T** term) and the state dipole moments $\Delta\mu_{\mathrm{eg}}$ (**D** term). Since the states with significant coupling to the ground state have small $\Delta\mu_{\mathrm{eg}}$ and few large couplings to other excited

states, these terms are at least an order of magnitude smaller than the **N** term. Because the **N** term has the dominant contribution in the SOS expression, $\mathrm{Re}(\gamma)$ is negative. This behavior is substantially different from that typically seen in π-conjugated systems, where large couplings between the excited states cause the **T** term to dominate and $\mathrm{Re}(\gamma)$ to be positive.[62−65]

Although our discussion has privileged PPh_4^+, the linear and NLO properties of all four members of the XPh_4 series are largely similar (Table 4). The energetic spacing of the first

Table 4. $\mathrm{Re}(\gamma)$ and Its Term Decomposition for the XPh_4 Series

central atom	$\mathrm{Re}(\gamma)$ ($\times 10^{-36}$ esu)			
	total	**D**	**T**	**N**
B^-	−44.2	0.7	5.8	−50.6
C	−42.0	1.0	6.8	−49.8
N^+	−39.3	1.7	6.2	−47.2
P^+	−39.8	1.1	2.1	−43.0

several frontier MOs is hardly affected by the identity of the central atom, so a similar mixing of many excitations in the low-lying excited states is observed. The four systems have similar NLO properties, with many states contributing significantly to $\mathrm{Re}(\gamma)$. The NLO properties are dependent on the spatial distribution and band-like energetic spacing of the first several frontier MOs, not on the identity of the central atom.

3.2. Experimental Results. *3.2.1. Linear Absorption Spectroscopy.* The linear absorption of PPh_4^+ dissolved in spectroscopic grade chloroform (Figure 3) exhibits a broad,
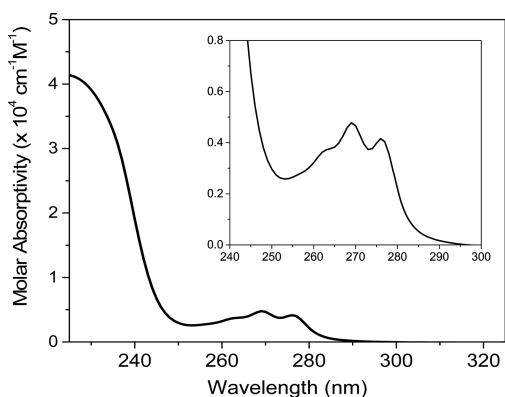

Figure 3. Molar absorptivity spectrum of PPh_4^+ dissolved in chloroform. The inset, having the same axis titles as the main figure, shows the molar absorptivity with the vertical and horizontal axes expanded.

multipeak absorption band between 250 and 280 nm (5.0−4.4 eV), with a maximum molar absorptivity of $0.42 \pm 0.04 \times 10^4$ cm^{-1} M^{-1} at 276 nm (4.49 eV). The molar absorptivity increases drastically at wavelengths shorter than 250 nm (5.0 eV); however, the absorption above 220 nm (5.6 eV) is not resolvable due to the high absorption of the solvent. Hence, the spectrophotometer cannot accurately subtract the transmission of the solvent from the solution at these wavelengths. The shape of the experimental absorption peak is consistent with the computed excited-state properties, which predict weak absorption into the first several excited states and much stronger absorption into higher-lying excited states.

The prepared solutions with concentrations ranging from 22 μM to ~91 mM in cuvette thicknesses from 10 μm to 1 cm showed no significant difference in the absorption shape in the 250−280 nm range, which indicates that there is no significant aggregation of the solute in this concentration range.

3.2.2. Nonlinear Spectroscopy. To perform the DA Z-scan measurements outlined in the Experimental Methodology section, a Ti:sapphire amplified laser (Clark-MXR CPA 2110) producing 1 mJ, ~150 fs (FWHM) pulses at a 1 kHz repetition rate pumps an optical parametric generator/amplifier (Light Conversion, Ltd., TOPAS-C) to generate pulses at 1300 nm for Z-scans. To characterize the minimum spot size and pulse-width of our input pulses, Z-scans were performed on two reference materials: fused silica and a bulk sample of GaAs. The Z-scan of fused silica gave an n_2 of $0.27 \pm 0.05 \times 10^{-15}$ cm^2/W which is in good agreement with literature values[66] and the Z-scan of GaAs gave a 2PA coefficient, α_2, of 27 ± 5 cm/GW also in good agreement with literature values and a two-band theoretical model.[67,68] These Z-scans of the reference materials gave the minimum spot size and pulse width of 22.5 μm (HW1/e^2 M) and 130 fs (FWHM), respectively.

To measure the signals from the DA Z-scan, a 91 mM concentration of PPh_4^+ in chloroform was placed in a 1 mm thick quartz cuvette in one arm of the DA Z-scan, while the pure solvent was placed in a closely matched 1 mm thick quartz cuvette in the other arm. Figure 4a shows the Z-scans of PPh_4^+ at a wavelength of 1300 nm using 3 different input pulse energies. At this wavelength, the excitation photon energy is ~5× below its linear absorption edge; hence, we can assume that the value of $\mathrm{Re}(\gamma)$ measured at this wavelength is close to its static (zero-frequency) limit. There was no observable Z-scan signal corresponding to nonlinear absorption, which suggests a negligible $\mathrm{Im}(\gamma)$. The n_2 coefficients are relatively constant over the range of input irradiances (see Figure 4b), indicating that there are no higher-order and/or cascaded NLR processes occurring. The error bars are deduced from the uncertainty in the pulse irradiance as well as the fitting errors to each scan. Therefore, we measure an n_2 of the solute at 1300 nm of $-0.11 \pm 0.03 \times 10^{-15}$ cm^2/W corresponding to an averaged molecular $\mathrm{Re}(\gamma) = -31 \pm 8 \times 10^{-36}$ esu (see eq 4). This value of $\mathrm{Re}(\gamma)$ is in very good agreement with the theoretical results shown in Table 4, both in terms of sign and magnitude. It must be borne in mind, however, that such a value is several orders of magnitude smaller than values recently reported for selenopyrylium polymethines.[12,69] Note that despite $\mathrm{Re}(\gamma)$ of PPh_4^+ being ~20× larger than the averaged $\mathrm{Re}(\gamma)$ of the solvent chloroform molecule, given that the concentration of the neat liquid is 12.47 M, the measured NLR signal from PPh_4^+ is ~7 times smaller than that of neat chloroform, and a factor of ~2 times smaller than that due to the quartz cuvette walls. Thus, the use of DA Z-scan was essential for these measurements.

4. CONCLUSIONS

Although a negative $\mathrm{Re}(\gamma)$ is advantageous for device applications, very few classes of molecules studied to date have negative $\mathrm{Re}(\gamma)$. Here, we present experimental evidence that molecules of the form XPh_4 have negative $\mathrm{Re}(\gamma)$ and provide a theoretical understanding of the NLO behavior in terms of the MOs and excited states. Experimentally, the accurate determination of nonlinearities far from resonances of molecules in solution has been problematic as the solvent nonlinearity typically dominates. The recent development of
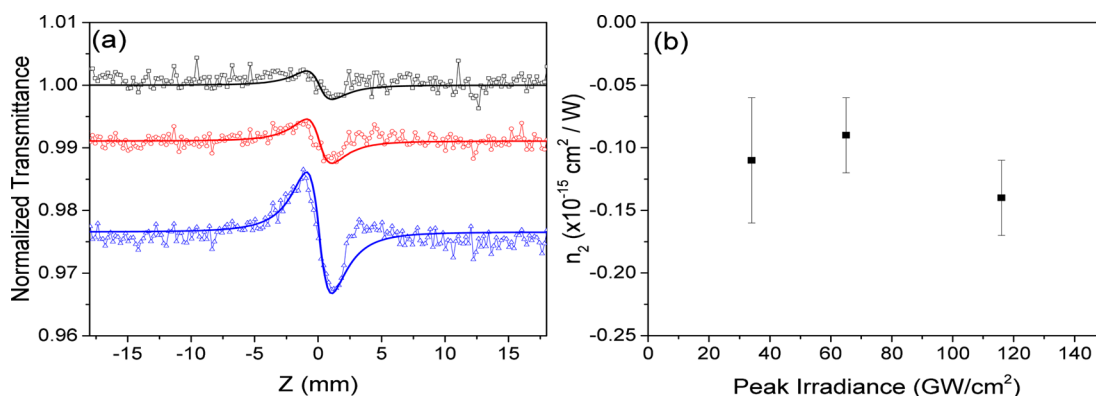
Figure 4. (a) DA Z-scans of a 91 mM concentration of PPh_4^+ at the laser wavelength of 1300 nm using different input pulse energies. (b) The values of the Z-scan fit with respect to the input peak irradiance. The open symbols in (a) represent the data, while the solid lines represent the fits to the data.

nonlinear differential techniques such as the dual-arm Z-scan has made it possible to overcome such limitations.

Unlike in typical linear conjugated systems, the NLO properties of the XPh_4 series depend on a band of several tens of low-lying excited states, of which several excited states are significantly coupled to the ground state. Since the π systems here are inherently three-dimensional, $Re(\gamma)$ is nearly isotropic, in contrast with typical linear π-conjugated systems that have significant nonlinearity primarily along a single molecular axis. Because of the complexity of the excited-state properties, the NLO properties must be understood in terms of the full SOS expression and cannot be simplified in terms of the commonly used essential-state model. Although the magnitude of $Re(\gamma)$ is relatively small, the discovery of a new molecular architecture offering the potential for a negative $Re(\gamma)$ provides new molecular design approaches to achieve a large negative $Re(\gamma)$ for device applications.

■ ASSOCIATED CONTENT

ⓢ Supporting Information

Additional details are provided about the computations of atomic charges, MOs, decomposition of transition dipole moments into orbital components, and state contributions to $Re(\gamma)$. The Supporting Information is available free of charge on the ACS Publications website at DOI: 10.1021/jacs.5b04377.

■ AUTHOR INFORMATION

Corresponding Authors
*ewvs@creol.ucf.edu
*jean-luc.bredas@kaust.edu.sa

Notes
The authors declare no competing financial interest.

■ ACKNOWLEDGMENTS

■ REFERENCES

(1) Kim, T.-D.; Kang, J.-W.; Luo, J.; Jang, S.-H.; Ka, J.-W.; Tucker, N.; Benedict, J. B.; Dalton, L.; Gray, T.; Overney, R. M.; Park, D. H.; Herman, W. N.; Jen, A. K. Y. *J. Am. Chem. Soc.* **2007**, *129*, 488.

(2) Dalton, L. R.; Benight, S. J.; Johnson, L. E.; Knorr, D. B.; Kosilkin, I.; Eichinger, B. E.; Robinson, B. H.; Jen, A. K. Y.; Overney, R. M. *Chem. Mater.* **2011**, *23*, 430.

(3) Dalton, L. R.; Sullivan, P. A.; Bale, D. H. *Chem. Rev.* **2010**, *110*, 25.

(4) Kwon, O. P.; Kwon, S.-J.; Jazbinsek, M.; Seo, J.-Y.; Kim, J.-T.; Seo, J.-I.; Lee, Y. S.; Yun, H.; Günter, P. *Chem. Mater.* **2011**, *23*, 239.

(5) Campagnola, P. J.; Loew, L. M. *Nat. Biotechnol.* **2003**, *21*, 1356.

(6) Zipfel, W. R.; Williams, R. M.; Christie, R.; Nikitin, A. Y.; Hyman, B. T.; Webb, W. W. *Proc. Natl. Acad. Sci. U.S.A.* **2003**, *100*, 7075.

(7) Albota, M. A.; Beljonne, D.; Brédas, J. L.; Ehrlich, J. E.; Fu, J. Y.; Heikal, A. A.; Hess, S.; Kogej, T.; Levin, M. D.; Marder, S. R.; McCord-Maughon, D.; Perry, J. W.; Röckel, H.; Rumi, M.; Subramaniam, G.; Webb, W. W.; Wu, X. L.; Xu, C. *Science* **1998**, *281*, 1653.

(8) Pawlicki, M.; Collins, H. A.; Denning, R. G.; Anderson, H. L. *Angew. Chem., Int. Ed.* **2009**, *48*, 3244.

(9) He, G. S.; Tan, L.-S.; Zheng, Q.; Prasad, P. N. *Chem. Rev.* **2008**, *108*, 1245.

(10) Spangler, C. W. *J. Mater. Chem.* **1999**, *9*, 2013.

(11) Hales, J. M.; Cozzuol, M.; Screen, T. E. O.; Anderson, H. L.; Perry, J. W. *Opt. Express* **2009**, *17*, 18478.

(12) Hales, J. M.; Matichak, J.; Barlow, S.; Ohira, S.; Yesudas, K.; Bredas, J. L.; Perry, J. W.; Marder, S. R. *Science* **2010**, *327*, 1485.

(13) Barlow, S.; Brédas, J. L.; Getmanenko, Y. A.; Gieseking, R. L.; Hales, J. M.; Kieu, K.; Kim, H.; Marder, S. R.; Norwood, R. A.; Perry, J. W.; Peyghambarian, N.; Risko, C.; Shahin, S.; Zhang, Y. *Mater. Horiz.* **2014**, *1*, 577.

(14) Stegeman, G. I.; Stolen, R. H. *J. Opt. Soc. Am. B* **1989**, *6*, 652.

(15) Chiao, R.; Garmire, E.; Townes, C. *Phys. Rev. Lett.* **1964**, *13*, 479.

(16) Kelley, P. L. *Phys. Rev. Lett.* **1965**, *15*, 1005.

(17) Lallemand, P.; Bloembergen, N. *Phys. Rev. Lett.* **1965**, *15*, 1010.

(18) Kashyap, R.; Blow, K. J. *Electron. Lett.* **1988**, *24*, 47.

(19) Bergano, N. S.; Davidson, C. R. *J. Lightwave Technol.* **1995**, *13*, 879.

(20) Essiambre, R. J.; Kramer, G.; Winzer, P. J.; Foschini, G. J.; Goebel, B. *J. Lightwave Technol.* **2010**, *28*, 662.

(21) Huy, M. C. P.; Baron, A.; Lebrun, S.; Frey, R.; Delaye, P. *J. Opt. Soc. Am. B* **2010**, *27*, 1886.

(22) Voronin, A. A.; Mitrokhin, V. P.; Ivanov, A. A.; Fedotov, A. B.; Sidorov-Biryukov, D. A.; Beloglazov, V. I.; Alfimov, M. V.; Ludvigsen, H.; Zheltikov, A. M. *Laser Phys. Lett.* **2010**, *7*, 46.

(23) Ippen, E. P.; Shank, C. V.; Gustafso, Tk *Appl. Phys. Lett.* **1974**, *24*, 190.

(24) Coen, S.; Chau, A. H. L.; Leonhardt, R.; Harvey, J. D.; Knight, J. C.; Wadsworth, W. J.; Russell, P. S. J. *J. Opt. Soc. Am. B* **2002**, *19*, 753.

(25) Bethge, J.; Husakou, A.; Mitschke, F.; Noack, F.; Griebner, U.; Steinmeyer, G.; Herrmann, J. *Opt. Express* **2010**, *18*, 6230.

(26) Marder, S. R.; Gorman, C. B.; Meyers, F.; Perry, J. W.; Bourhill, G.; Brédas, J. L.; Pierce, B. M. *Science* **1994**, *265*, 632.

(27) Meyers, F.; Marder, S. R.; Pierce, B. M.; Bredas, J. L. *J. Am. Chem. Soc.* **1994**, *116*, 10703.

(28) Yang, M.; Jiang, Y. *Phys. Chem. Chem. Phys.* **2001**, *3*, 4213.

(29) Guo, S.-L.; Li, T.-P.; Wang, T.-B.; Liu, Z.-S.; Cao, T.-D. *Opt. Mater.* **2007**, *29*, 494.

(30) Prabhakar, C.; Yesudas, K.; Bhanuprakash, K.; Jayathirtha Rao, V.; Sai Santosh Kumar, R.; Narayana Rao, D. *J. Phys. Chem. C* **2008**, *112*, 13272.

(31) Dirk, C. W.; Herndon, W. C.; Cervantes-Lee, F.; Selnau, H.; Martinez, S.; Kalamegham, P.; Tan, A.; Campos, G.; Velez, M.; Zyss, J.; Ledoux, I.; Cheng, L.-T. *J. Am. Chem. Soc.* **1995**, *117*, 2214.

(32) Whittall, I. R.; Humphrey, M. G. *Organometallics* **1995**, *14*, 5493.

(33) Letard, J.-F.; Montant, S.; Guionneau, P.; Martin, P.; Le Calvez, A.; Freysz, E.; Chasseau, D.; Lapouyade, R.; Kahn, O. *Chem. Commun.* **1997**, *1997*, 745.

(34) Diaz-Garcia, M. A.; Ledoux, I.; Duro, J. A.; Torres, T.; Agullo-Lopez, F.; Zyss, J. *J. Phys. Chem.* **1994**, *98*, 8761.

(35) DeSalvo, R.; Said, A. A.; Hagan, D. J.; VanStryland, E. W.; SheikBahae, M. *IEEE J. Quantum Electron.* **1996**, *32*, 1324.

(36) Tanaka, K. *J. Mater. Sci.: Mater. Electron.* **2005**, *16*, 633.

(37) Orr, B. J.; Ward, J. F. *Mol. Phys.* **1971**, *20*, 513.

(38) Pierce, B. M. *Proc. SPIE* **1991**, *1560*, 148.

(39) Garito, A. F.; Teng, C. C. *Proc. SPIE* **1986**, *0613*, 146.

(40) Helfin, J. R.; Garito, A. F. In *Electroresponsive Molecular and Polymeric Systems*; Skotheim, T. A., Ed.; Marcel Dekker Inc.: New York, 1991; p 1.

(41) Pierce, B. M. In *Molecular and Biomolecular Electronics*; American Chemical Society: Washington DC, 1994; Vol. *240*, p 243.

(42) Dirk, C. W.; Cheng, L.-T.; Kuzyk, M. G. *Int. J. Quantum Chem.* **1992**, *43*, 27.

(43) Kuzyk, M.; Dirk, C. *Phys. Rev. A* **1990**, *41*, 5098.

(44) Marder, S. R.; Perry, J. W.; Bourhill, G.; Gorman, C. B.; Tiemann, B. G.; Mansour, K. *Science* **1993**, *261*, 186.

(45) Wernke, W.; Pfeiffer, M.; Johr, T.; Lau, A.; Grahn, W.; Johannes, H.-H.; Dahne, L. *Chem. Phys.* **1997**, *216*, 337.

(46) Mukhopadhyay, S.; Risko, C.; Marder, S. R.; Brédas, J.-L. *Chem. Sci.* **2012**, *3*, 3103.

(47) Chai, J.-D.; Head-Gordon, M. *Phys. Chem. Chem. Phys.* **2008**, *10*, 6615.

(48) Chai, J.-D.; Head-Gordon, M. *J. Chem. Phys.* **2008**, *128*, 084106.

(49) Dunning, T. H. *J. Chem. Phys.* **1989**, *90*, 1007.

(50) Frisch, M. J.; Trucks, G. W.; Schlegel, H. B.; Scuseria, G. E.; Robb, M. A.; Cheeseman, J. R.; Scalmani, G.; Barone, V.; Mennucci, B.; Petersson, G. A.; Nakatsuji, H.; Caricato, M.; Li, X.; Hratchian, H. P.; Izmaylov, A. F.; Bloino, J.; Zheng, G.; Sonnenberg, J. L.; Hada, M.; Ehara, M.; Toyota, K.; Fukuda, R.; Hasegawa, J.; Ishida, M.; Nakajima, T.; Honda, Y.; Kitao, O.; Nakai, H.; Vreven, T.; Montgomery, J. A., Jr.; Peralta, J. E.; Ogliaro, F.; Bearpark, M.; Heyd, J. J.; Brothers, E.; Kudin, K. N.; Staroverov, V. N.; Keith, T.; Kobayashi, R.; Normand, J.; Raghavachari, K.; Rendell, A.; Burant, J. C.; Iyengar, S. S.; Tomasi, J.; Cossi, M.; Rega, N.; Millam, J. M.; Klene, M.; Knox, J. E.; Cross, J. B.; Bakken, V.; Adamo, C.; Jaramillo, J.; Gomperts, R.; Stratmann, R. E.; Yazyev, O.; Austin, A. J.; Cammi, R.; Pomelli, C.; Ochterski, J. W.; Martin, R. L.; Morokuma, K.; Zakrzewski, V. G.; Voth, G. A.; Salvador, P.; Dannenberg, J. J.; Dapprich, S.; Daniels, A. D.; Farkas, O.; Foresman, J. B.; Ortiz, J. V.; Cioslowski, J.; Fox, D. J. *Gaussian 09*, revision B.01; Gaussian, Inc.: Wallingford, CT, 2010.

(51) Zojer, E.; Beljonne, D.; Kogej, T.; Vogel, H.; Marder, S. R.; Perry, J. W.; Brédas, J. L. *J. Chem. Phys.* **2002**, *116*, 3646.

(52) Ohira, S.; Hales, J. M.; Thorley, K. J.; Anderson, H. L.; Perry, J. W.; Bredas, J. L. *J. Am. Chem. Soc.* **2009**, *131*, 6099.

(53) Zojer, E.; Beljonne, D.; Pacher, P.; Bredas, J. L. *Chem.—Eur. J.* **2004**, *10*, 2668.

(54) Zojer, E.; Wenseleers, W.; Halik, M.; Grasso, C.; Barlow, S.; Perry, J. W.; Marder, S. R.; Brédas, J.-L. *ChemPhysChem* **2004**, *5*, 982.

(55) Gieseking, R. L.; Mukhopadhyay, S.; Risko, C.; Brédas, J.-L. *ACS Photonics* **2014**, *1*, 261.

(56) Cave, R. J.; Davidson, E. R. *J. Phys. Chem.* **1988**, *92*, 614.

(57) Cave, R. J.; Davidson, E. R. *J. Phys. Chem.* **1987**, *91*, 4481.

(58) Ferdinandus, M. R.; Reichert, M.; Ensley, T. R.; Hu, H.; Fishman, D. A.; Webster, S.; Hagan, D. J.; Van Stryland, E. W. *Opt. Mater. Express* **2012**, *2*, 1776.

(59) Sheik-Bahae, M.; Said, A. A.; Wei, T.-H.; Hagan, D. J.; Van Stryland, E. W. *IEEE J. Quantum Electron.* **1990**, *26*, 760.

(60) In charged systems, the state dipole moments depend on the choice of the origin; however, the differences between state dipole moments do not so long as the same origin is used for both state dipole moments. We select the location of the central atom X as the origin; since the molecules have S_4 symmetry, this is also the center of charge.

(61) The orbital components of the transition dipole moments discussed here include a quantum prefactor of $\sqrt{2}$ because the INDO/CI approach uses singlet-adapted states.

(62) Nalwa, H. S. *Adv. Mater.* **1993**, *5*, 341.

(63) Tykwinski, R. R.; Gubler, U.; Martin, R. E.; Diederich, F.; Bosshard, C.; Gunter, P. *J. Phys. Chem. B* **1998**, *102*, 4451.

(64) Gubler, U.; Bosshard, C. *Adv. Polym. Sci.* **2002**, *158*, 123.

(65) Bredas, J. L.; Adant, C.; Tackx, P.; Persoons, A.; Pierce, B. M. *Chem. Rev.* **1994**, *94*, 243.

(66) Milam, D. *Appl. Opt.* **1998**, *37*, 546.

(67) Hurlbut, W. C.; Lee, Y.-S.; Vodopyanov, K. L.; Kuo, P. S.; Fejer, M. M. *Opt. Lett.* **2007**, *32*, 668.

(68) Van Stryland, E. W.; Woodall, M. A.; Vanherzeele, H.; Soileau, M. J. *Opt. Lett.* **1985**, *10*, 490.

(69) Because ω_{exc}/ω_{ge} is relatively large in the selenopyrylium polymethines, Re(γ) is enhanced relative to the static (zero-frequency) limit due to preresonant enhancement. The computed Re$(\gamma)_{stat}$ for the Se-3C is approximately 28 times larger than that of PPh$_4^+$, and the larger selenopyrylium polymethines have even larger Re$(\gamma)_{stat}$ values.